Vortex Imaging in the π-Band of Magnesium Diboride

M. R. Eskildsen[1],* M. Kugler[1], S. Tanaka[1,2], J. Jun[3], S. M. Kazakov[3], J. Karpinski[3], and Ø. Fischer[1]
[1] *DPMC, University of Geneva, 24 Quai E.-Ansermet, CH-1211 Genève 4, Switzerland*
[2] *Department of Physics, Saga University, Saga 840-8502, Japan*
[3] *Solid State Physics Laboratory, ETH, CH-8093 Zürich, Switzerland*
(Dated: February 1, 2008)

We report scanning tunneling spectroscopy imaging of the vortex lattice in single crystalline MgB_2. By tunneling parallel to the c-axis, a single superconducting gap ($\Delta = 2.2$ meV) associated with the π-band is observed. The vortices in the π-band have a large core size compared to estimates based on H_{c2}, and show an absence of localized states in the core. Furthermore, superconductivity between the vortices is rapidly suppressed by an applied field. These results suggest that superconductivity in the π-band is, at least partially, induced by the intrinsically superconducting σ-band.

PACS numbers: PACS numbers: 74.50.+r, 74.70.Ad,74.60.Ec

Superconductivity in magnesium diboride (MgB_2) with a remarkably high $T_c = 39$ K was recently reported by Nagamatsu *et al.* [1]. Since then, great attention has been directed towards understanding the detailed nature of superconductivity in this material, an in particular whether this is a one- or two-gap superconductor. Two-gap superconductivity was predicted theoretically [2, 3], and is now supported by an increasing number of experimental reports [4, 5, 6, 7, 8, 9, 10, 11, 12]. Two-gap or two-band superconductivity was first studied in the fifties [13], and has now found renewed relevance in MgB_2. In addition, and contrary to many materials or alloys studied earlier, the two bands in MgB_2 have roughly equal filling factor, opening the possibility for interesting new phenomena. However, the exact microscopic details are still largely unexplored. An ideal way to address this issue is by local spectroscopic investigations of the mixed state, which has become possible with the recent availability of high quality MgB_2 single crystals.

In this Letter we report on scanning tunneling spectroscopy (STS) measurements on single crystal MgB_2, including the first vortex imaging in this material. Tunneling parallel to the c-axis, we are able to selectively measure only the π-band [14], in which the vortices are found to have a number of remarkable properties: An absence of localized states, a very large vortex core size compared to the estimate based on H_{c2}, and a strong core overlap.

The STS experiments were performed using a home built scanning tunneling microscope (STM) installed in a ^{3}He, ultra high vacuum cryostat holding a 14 T magnet [15]. The measurements were done on the surface of an as grown single crystal, using electrochemically etched iridium tips. Single crystals of MgB_2 were grown using a high pressure method described elsewhere [16], yielding platelike samples with the surface normal parallel to the crystalline c-axis. The surface of the crystals are roughly 0.25×0.25 mm^2, and the thickness of the order of microns. The critical temperature is typically $T_c \approx 38 - 39$ K, with a sharp transition, $\Delta T_c = 0.5$ K, measured by SQUID magnetometry [17]. The STS experiments were done with both the tunneling direction and the applied magnetic field parallel to the c-axis, and the differential conductivity measured using a standard AC lock-in technique. In this configuration the upper critical field extrapolates to $H_{c2}(T = 0\mathrm{K}) = 3.1$ T [17]. Using the Ginzburg-Landau (GL) expression for $H_{c2} = \phi_0/(2\pi\xi^2)$, where $\phi_0 = h/2e$ is the flux quantum, yields a coherence length, $\xi_{GL} = 10$ nm. An estimate of the mean free path, based on the measured residual resistivity [18] and specific heat [11], and the calculated Fermi velocity [14], gives $l = 50 - 100$ nm, indicating that the samples are in the clean limit.

We will first focus on the zero-field electronic spectrum of MgB_2. The observation of a single or double gaps depends on the orientation of the sample, as shown by Iavarone *et al.*, who investigated a number of single grains with different, but unknown absolute orientations [12]. Here we report the first STS measurements on a MgB_2 single crystal, which allow a correlation between the tunneling direction and the observed gap(s). In Fig. 1 we show a superconducting spectrum obtained at a temperature of 320 mK. This is an average of 40 spectra obtained along a 100 nm path, which shows perfect homogeneity. One observes a single gap with coherence peaks at ± 2.5 meV, and additional weak shoulders at ± 6 meV, as indicated by the arrows. In addition, the flat region around the Fermi energy proves the absence of nodes in the gap, and hence that MgB_2 is a s-wave superconductor. The very low zero bias conductance indicates a high quality tunnel junction and a low noise level. True vacuum tunneling conditions were assured by varying the tunnel resistance, R_t, and verifying that the spectra normalized to the conductance outside the superconducting gap collapse on a single curve. The spectrum can be fitted by the BCS expression for the density of states (DOS), including a finite quasiparticle lifetime, Γ [19], and an experimental broadening. The result of the fit is shown in Fig. 1 and yields a superconducting gap, $\Delta = 2.2$ meV. We have studied the temperature depen-

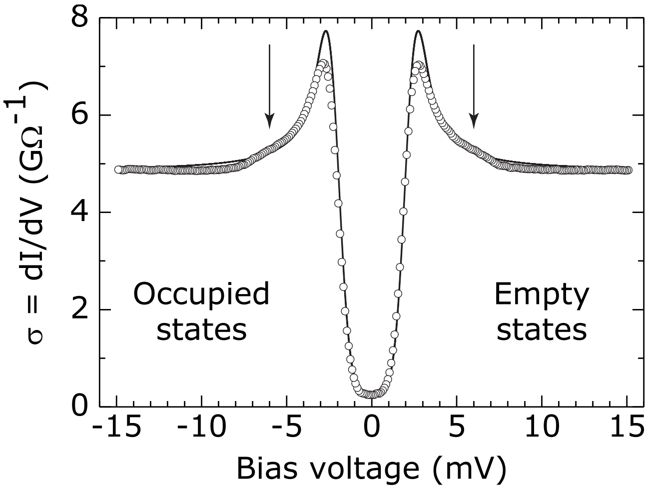

FIG. 1: Zero-field superconducting spectrum of MgB_2 at 320 mK for tunneling parallel to the c-axis and a tunnel resistance, $R_t = 0.2$ GΩ ($U = 0.1$ V; $I = 0.5$ nA). The bias voltage is applied to the sample. Clear coherence peaks are seen at ± 2.5 meV, and additional weak shoulders at ± 6 meV as indicated by the arrows. The line is a fit to the Dynes DOS [19] ($\Delta = 2.2$ meV, $\Gamma = 0.1$ meV) convoluted by a gaussian of width 0.5 meV RMS to account for experimental smearing, including the use of a finite AC excitation (0.4 mV RMS).

dence of the superconducting gap and found excellent agreement with the BCS $\Delta(T)$.

The fact that only one superconducting gap is observed for tunneling parallel to the c-axis, is explained theoretically by calculations of the Fermi surface and an analysis of how tunneling along different directions is coupled to the different bands. The Fermi surface of MgB_2 falls into two distinct sheets: One is derived from σ-antibonding states of the boron p_{xy} orbitals and is a two-dimensional cylindrical sheet parallel to c^*, while the other consists of π-bonding and antibonding states of the boron p_z orbitals and is three-dimensional [2, 3, 20]. The tunneling matrix element is different for the two bands, and depends on the tunneling direction. The c-axis tunneling probability into the σ-band is ten times smaller than into the π-band [14]. Furthermore, the calculated superconducting gap sizes for the two different Fermi surfaces are different, with $\Delta_\sigma \approx 7$ meV, and $\Delta_\pi \approx 2$ meV [3]. This is in agreement with our results, where one gap with $\Delta = \Delta_\pi = 2.2$ meV is observed, with the shoulders at 6 meV being a remnant of Δ_σ. The selective sensitivity to Δ_π turns out to be particularly useful, as we will show in the following.

We now turn to measurements in an applied magnetic field. In a type-II superconductor such as MgB_2, a magnetic field penetrates into the sample in the form of vortices each carrying one flux quantum, which are generally arranged in a periodic array: the vortex lattice. In the core of each vortex, superconductivity is suppressed within a radius roughly given by the coherence length, ξ. The vortex spacing is determined by the applied field and the flux quantization, and in the case of a hexagonal vortex lattice it is $d = (2/\sqrt{3}\ \phi_0/H)^{1/2}$. The magnetic fields were applied at 2 K, and the system allowed to stabilize for at least a few hours. After this time no vortex motion was observed, indicating a fast relaxation and hence low vortex pinning in the crystal.

In Fig. 2a we show a STS image of a single vortex induced by a field of 0.05 T. The image was obtained by measuring the differential conductance at zero bias and normalizing this to the conductance at the coherence peak. Low values of the normalized conductance correpond to superconducting areas, and high values to the vortex cores. The low field is equivalent to a separation, $d = 220$ nm $\gg \xi$. The vortices can therefore be considered as isolated from each other. Such isolated vortices are expected to contain localized quasiparticle states, which should show up as a zero bias conductance (ZBC) peak at the vortex centre [21], provided that the sample is sufficiently clean to prevent these to be smeared out by scattering. We have measured the evolution of the spectra at a large number of positions along a trace across the vortex core as shown in Fig. 2c. Contrary to expectations, we find that the normalized ZBC increases to one with no indication of any localized states. Instead, the spectra in the centre of the vortex are *absolutely flat*, with no excess spectral weight at or close to zero bias. This absence of localized states is striking, considering that $l = 5 - 10 \times \xi_{GL}$. However, as we will show below, the coherence length in the π-band is approximately 50 nm. This is much larger that the estimate based on H_{c2}, and equal to only one to two times the mean free path. Nonetheless, systematic studies of $Nb_{1-x}Ta_xSe_2$ with $x = 0 - 0.2$, showed that even for $\xi/l \approx 1$ some excess weight close to zero bias was observed [22]. In parallel to STS imaging, STM topographic images were recorded (not shown), which revealed a flat surface with a RMS roughness of 6 Å over the whole image area.

Before analyzing the vortex profile in detail, we will consider the situation at higher fields. In Fig. 2b we show the STS image of the hexagonal vortex lattice observed at 0.2 T. We notice that the normalized ZBC between the vortices, is now enhanced with respect to the value far from the single vortex at 0.05 T. This increase of the "bulk" ZBC is unusual at such a modest field, only about 7% of H_{c2}. To elucidate this behaviour, "bulk" spectra for fields between zero and 0.5 T are shown in Fig. 2d. It is clear that even modest fields rapidly suppress superconductivity in the region between the vortices. This is seen both by an increase of the ZBC and by a suppression of the coherence peaks outside the vortex cores, which one would only expect for fields close to H_{c2}, corresponding to a significant core overlap. This is consistent with earlier point contact spectroscopy measurements [5], with the addition that we resolve the local behaviour on a microscopic scale.

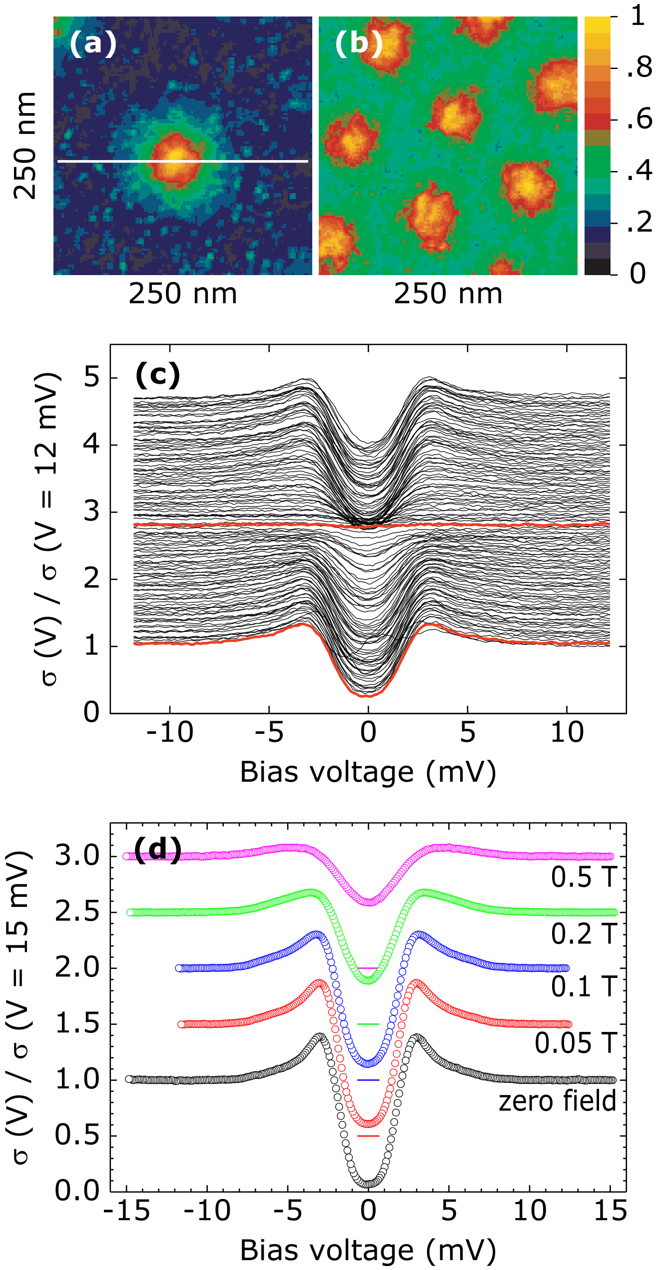

FIG. 2: (color) Vortices in MgB_2. Top: 250×250 nm^2 false color spectroscopic images of a single vortex induced by an applied field of 0.05 T (a), and the vortex lattice at 0.2 T (b). In both cases the tunnel resistance was, $R_t = 0.4$ GΩ ($U = 0.2$ V; $I = 0.5$ nA). The conductance is normalized to respectively 2.9 meV (0.05 T) and 3.9 meV (0.2 T). (c): 250 nm trace across the single vortex indicated by the white line in (a), with spectra recorded each 2 nm. Each spectrum is normalized to the conductivity at 12 meV, and $R_t = 0.4$ GΩ. A spectrum at the vortex centre together with one far from the vortex core have been highlighted in red for clarity. (d): Normalized spectra measured in zero field, and between the vortices for fields between 0.05 T and 0.5 T ($R_t = 0.2$ GΩ). Each subsequent spectrum is offset by 0.5 with respect to the previous one. The bars at zero bias indicate the respective zero conductivity for the offset spectra. All measurements in this figure were performed at 2 K.

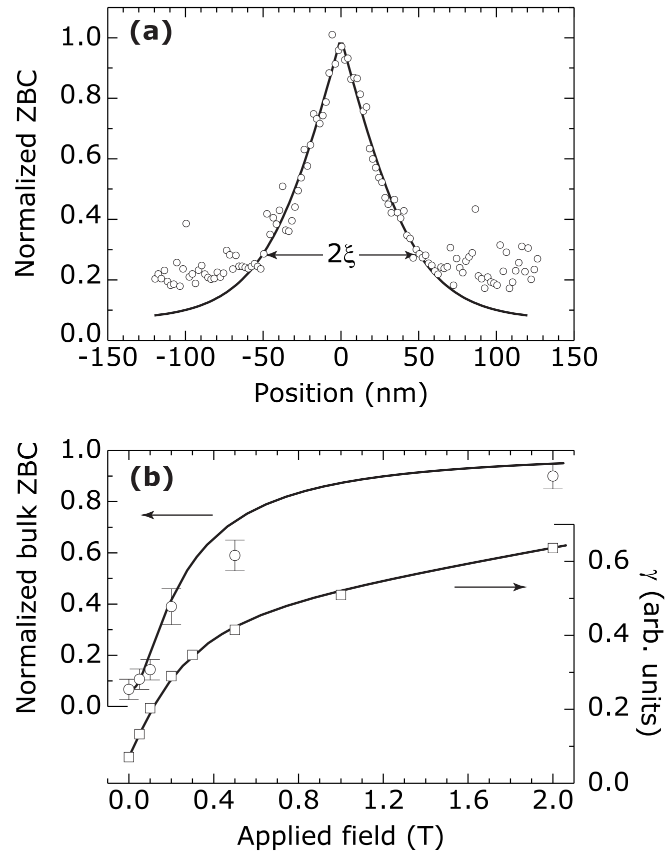

FIG. 3: Vortex size and core overlap. (a): Normalized zero bias conductance versus distance from the centre, for the isolated vortex shown in Fig. 2a. The line is a fit to eq. (1) in the text. (b): Calculated "bulk" ZBC (left axis) and electronic specific heat, γ, for $\gamma_n^\pi/\gamma_n^\sigma = 0.55/0.45$ (right axis). The calculated values are compared to respectively the measured bulk ZBC (circles), and specific heat measurements on polycrystalline samples (squares) [11].

We now return to the single vortex measurement. In Fig. 3a, we have plotted the normalized ZBC, $\sigma'(x,0)$, for the vortex trace measured at 0.05 T. It is immediately clear that the spatial extension of the vortex core is much larger than the 10 nm estimated from H_{c2}. Somewhat surprisingly, we find that the ZBC profile can be fitted by one minus the GL expression for the superconducting order parameter:

$$\sigma'(x,0) = \sigma'_0 + (1-\sigma'_0) \times (1 - \tanh x/\xi), \qquad (1)$$

where $\sigma'_0 = 0.068$ is the normalized ZBC measured in zero field. The fit, shown in Fig. 3a, yields a coherence length, $\xi = \xi_\pi = 49.6 \pm 0.9$ nm. Using the GL expression to calculate the upper critical field with this value of the coherence length, yields $H'_{c2} = 0.13$ T. At 0.2 T we hence find ourselves in the bizarre situation of imaging the vortex lattice above the nominal H'_{c2}. Additional vortex lattice imaging has been performed as high as 0.5 T.

This apparent paradox can be reconciled if one assumes that superconductivity in the π-band is induced by the σ-band, either by interband scattering, or Cooper pair tunneling [13, 23]. This means that isolated the π-band would either be non-superconducting or have a very low upper critical field. Consequently the observed behaviour reflects the state in the σ-band by an interband proximity effect, along the lines of recent theoretical work [23]. The vanishing of $\Delta_\pi(T)$ at the bulk T_c further supports this conclusion. Finally, it is also consistent with estimates of the coherence lengths, using the BCS expression $\xi_0 = \hbar v_F/(\pi\Delta(0))$ and considering each band separately. Taking the calculated average Fermi velocity in the ab-plane for the π-band, $v_F^\pi = 5.35 \times 10^5$ m/s [14], and the measured gap value $\Delta_\pi = 2.2$ meV we get $\xi_0^\pi = 51$ nm, in excellent agreement with ξ_π obtained from the vortex profile. A similar analysis for the σ-band, using $v_F^\sigma = 4.4 \times 10^5$ m/s [14] and $\Delta_\sigma = 7.1$ meV [12] yields $\xi_0^\sigma = 13$ nm. This agrees with the coherence length obtained from H_{c2}, and reinforces the conclusion that it is mainly the σ-band which is responsible for superconductivity in MgB_2, and thus determins the macroscopic parameters T_c and H_{c2}.

As described above, it is the transfer from the σ-band that makes superconductivity in the π-band possible, despite a strong vortex core overlap already at very low magnetic fields. Constructing a simple model for the core overlap in the π-band by

$$\sigma'(\boldsymbol{r}, 0) = \sigma'_0 + (1 - \sigma'_0) \times \left(1 - \Pi_i \tanh \frac{|\boldsymbol{r} - \boldsymbol{r}_i|}{\xi_\pi}\right), \quad (2)$$

where $\boldsymbol{r}_i$ are the vortex positions for a hexagonal lattice with a density corresponding to the applied field, we can calculate the ZBC at any position in the vortex lattice unit cell. In Fig. 3b we compare the calculated conductivity at the midpoint between three vortices with the measured bulk ZBC. This shows a very good agreement, especially taking into account that there are no free parameters in the calculation: ξ_π is determined from the vortex profile, and σ'_0 from the zero field measurement. The vortex core overlap also explains the, strongly nonlinear field dependence of the electronic specific heat, γ [4, 11]. In strongly type-II superconductors core overlap is usually negligible, with each vortex creating the same number of quasiparticles at the Fermi surface, and hence contributing by the same amount to the specific heat. In that case $\gamma = \gamma_n\ H/H_{c2}$, where γ_n is the electronic specific heat in the normal state. However, in the case of MgB_2, with strong core overlap in the π-band, the isolated vortex assumption is violated. Instead, one can calculate the contribution from the π-band, simply by averaging the normalized ZBC in one vortex lattice unit cell, $\gamma_\pi = \gamma_n^\pi\ \langle\sigma'(\boldsymbol{r}, 0)\rangle$ [23]. On the other hand, the σ-band can be described by the usual linear field dependence $\gamma_\sigma = \gamma_n^\sigma\ H/H_{c2}$. Adding the terms gives $\gamma = \gamma_\pi + \gamma_\sigma$, where $\gamma_n^\pi/\gamma_n^\sigma$ is the relative weigth of the two bands. The calculated field dependence of γ is shown in Fig. 3b, in perfect agreement with the measured specific heat for polycrystalline MgB_2 [11], using $\gamma_n^\pi/\gamma_n^\sigma = 0.55/0.45$.

In summary, we have presented STS data on the π-band in MgB_2, including the first vortex imaging in this material. We have demonstrated the absence of localized states in the vortex core, a very large vortex core size and a strong core overlap. The data presents a striking experimental demonstration of the fundamentally different microscopic properties of the two bands in MgB_2.

We acknowledge valuable discussions and communication of data prior to publication with F. Bouquet, Y. Wang and A. Junod, and thank B. W. Hoogenboom and I. Maggio-Aprile for sharing their experience in STM/STS. This work was supported by Swiss National Science Foundation. M.R.E. has received support from the Christian and Anny Wendelbo foundation and from The Danish Natural Science Research Council.

* Electronic address: morten.eskildsen@physics.unige.ch

[1] J. Nagamatsu *et al.*, Nature (London) **410**, 63 (2001).
[2] A. Y. Liu, I. I. Mazin and J. Kortus, Phys. Rev. Lett. **87**, 087005 (2001).
[3] H. J. Choi *et al.*, cond-mat/0111183.
[4] Y. Wang, T. Plackowski and A. Junod, Physica (Amsterdam) **355C**, 179 (2001).
[5] P. Szabó *et al.*, Phys. Rev. Lett. **87**, 137005 (2001).
[6] X. K. Chen *et al.*, Phys. Rev. Lett. **87**, 157002 (2001).
[7] F. Giubileo *et al.*, Phys. Rev. Lett. **87**, 177008 (2001).
[8] For a review of the earliest work see e.g. C. Buzea and T. Yamashita, Supercond., Science & Technology **14**, R115 (2001).
[9] F. Bouquet *et al.*, Europhys. Lett. **56**, 856 (2001).
[10] H. Schmidt *et al.*, Phys. Rev. Lett. **88**, 127002 (2002).
[11] A. Junod *et al.*, in *Studies of High Temperature Superconductors*, edited by A. Narlikar, **38**, 179 (Nova Publishers, Commack (N.Y.), 2002).
[12] M. Iavarone *et al.*, cond-mat/0203329.
[13] For a review see G. Gladstone, M. A. Jensen and J. R. Schrieffer, in Superconductivity, edited by R. D. Parks, **2**, 665 (Marcel Dekker, New York, 1969).
[14] A. Brinkman *et al.*, cond-mat/0111115.
[15] M. Kugler *et al.*, Rev. Sci. Instrum. **71**, 1475 (2000).
[16] J. Karpinski *et al.*, in preparation.
[17] M. Angst *et al*, Phys. Rev. Lett. **88**, 167004 (2002).
[18] A. V. Sologubenko *et al.*, cond-mat/0112191.
[19] R. C. Dynes, V. Narayanamurti and J. P. Garno, Phys. Rev. Lett. **41**, 1509 (1978).
[20] J. Kortus *et al.*, Phys. Rev. Lett. **86**, 4656 (2001).
[21] H. F. Hess *et al.*, Phys. Rev. Lett. **62**, 214 (1989); F. Gygi and M. Schlüter, Phys. Rev. B **43**, 7609 (1991).
[22] Ch. Renner *et al.*, Phys. Rev. Lett. **67**, 1650 (1991).
[23] N. Nakai, M. Ichioka and K. Machida, J. Phys. Soc. Japan **71**, L23 (2002).